



# Typical meteorological conditions associated with extreme nitrogen dioxide (NO<sub>2</sub>) pollution events over Scandinavia

Manu Anna Thomas and Abhay Devasthale

Research and development department, Swedish Meteorological and Hydrological Institute (SMHI), Folkborgsvägen 17, 60176 Norrköping, Sweden

Correspondence to: M. A. Thomas (manu.thomas@smhi.se)

Received: 3 December 2016 – Discussion started: 21 February 2017

Revised: 31 August 2017 – Accepted: 9 September 2017 – Published: 12 October 2017

**Abstract.** Characterizing typical meteorological conditions associated with extreme pollution events helps to better understand the role of local meteorology in governing the transport and distribution of pollutants in the atmosphere. The knowledge of their co-variability could further help to evaluate and constrain chemistry transport models. Hence, in this study, we investigate the statistical linkages between extreme nitrogen dioxide (NO<sub>2</sub>) pollution events and meteorology over Scandinavia using observational and reanalysis data. It is observed that the south-westerly winds dominated during extreme events, accounting for 50–65 % of the total events depending on the season, while the second largest annual occurrence was from south-easterly winds, accounting for 17 % of total events. The specific humidity anomalies showed an influx of warmer and moisture-laden air masses over Scandinavia in the free troposphere. Two distinct modes in the persistency of circulation patterns are observed. The first mode lasts for 1–2 days, dominated by south-easterly winds that prevailed during 78 % of total extreme events in that mode, while the second mode lasted for 3–5 days, dominated by south-westerly winds that prevailed during 86 % of the events. The combined analysis of circulation patterns, their persistency, and associated changes in humidity and clouds suggests that NO<sub>2</sub> extreme events over Scandinavia occur mainly due to long-range transport from the southern latitudes.

## 1 Introduction

Nitrogen dioxide (NO<sub>2</sub>) is one of the highly reactive gases of the nitrogen oxides (NO<sub>x</sub>) family. The major sources of NO<sub>2</sub> are fuel combustion in motor vehicles, industrial boilers, and emissions from soil and agricultural biomass burning. Natural sources of NO<sub>2</sub> are lightning and forest fires. Recent studies indicate increasing trends in NO<sub>2</sub> in developing countries and decreasing trends in developed countries as a result of environmental regulation policies (Richter et al., 2005; Zhang et al., 2007; van der A et al., 2008; Schneider et al., 2015; Geddes et al., 2016). NO<sub>2</sub> is an oxidizing agent resulting in the corrosive nitric acid and plays an important role in aiding the formation of ozone. It can also contribute to the formation of particulate matter and secondary organic particles through photochemical reactions. Increased NO<sub>x</sub> concentrations not only severely affect human physical health through reduced lung function but also affect aquatic ecosystems through acid deposition and eutrophication of soil and water (Sjöberg et al., 2004; Klingberg et al., 2009; Bellandar et al., 2012; Gustafsson et al., 2014; Nilsson Sommar et al., 2014; Oudin et al., 2016; Taj et al., 2016). Lamarque et al. (2013) based on the multi-model intercomparison assessed increases in regional nitrogen deposition by up to 30–50 % from RCP 2.6 to RCP 8.5. According to the 4th IPCC Assessment Report, the total global NO<sub>x</sub> emissions have increased from a pre-industrial value of 12 Tg N yr<sup>-1</sup> to between 42 and 47 Tg N yr<sup>-1</sup> in 2000. The most recent study by Miyazaki et al. (2017) estimated 10-year (2005–2014) global total surface NO<sub>x</sub> emissions of 48.4 Tg N yr<sup>-1</sup> with an increase of 29, 26, and 20 % per decade increase respectively over India, China and the Middle East and a decrease of 38, 8.2, and 8.8 % respectively over the United States, southern

Africa, and western Europe. In heavily polluted areas, NO<sub>2</sub> can also have noticeable impact on the local radiation budget (Vasilkov et al., 2009).

Compared to other pollutants such as carbon monoxide (CO) that has a life span of weeks to a few months, NO<sub>2</sub> has a relatively shorter lifetime in the atmosphere and ranges typically from a couple of hours in the boundary layer up to a few days in the upper troposphere (Beirle et al., 2011). Therefore, NO<sub>2</sub> can be typically associated with short-range transport events. For long-range transport (LRT) or intercontinental transport of pollutants, NO<sub>2</sub> in particular, to occur, the associated weather systems need to be linked with stronger winds and rapid convective–advective events such as cyclones or warm conveyor belts (WCBs) that can lift air masses from their source regions up into the free troposphere and be transported across the oceans (Eckhardt et al., 2003; Stohl et al., 2003). Due to lower concentrations of radical species in the free troposphere, the reaction with NO<sub>2</sub> is limited. Zien et al. (2014) identified about 3800 LRT events of NO<sub>2</sub> during a 5-year period from the major pollution hotspots such as the east coast of North America, central Europe, China, and South America, predominantly during autumn and winter months.

There have been several studies reporting individual LRT events of NO<sub>2</sub>. To mention a few, Stohl et al. (2003) in a study explained “intercontinental express highways” being responsible for almost 60 % of the total intercontinental transport of pollutants from across the Atlantic to Europe, resulting in an increase of average European winter NO<sub>x</sub> mixing ratios of about 2–3 pptv. In yet another study, Schaub et al. (2005) demonstrated that at least 50 % of the NO<sub>2</sub> recorded at an alpine region was advected via a frontal system from the Ruhr area in central Germany in February 2001. Donnelly et al. (2015) reported that easterly air masses during winter resulted in increased NO<sub>2</sub> concentrations in the urban and rural sites in Ireland. LRT of NO<sub>x</sub> across the Indian Ocean from South Africa to Australia in May 1998 was reported by Wenig et al. (2003).

The Nordic countries often lie at the receiving end of short-range pollutant transport from northern Europe or they are a part of a much larger transit pathway of eventual long-range transport to the Arctic, originating from either Europe or North America. To what extent such a transport from the southerly latitudes affects the characteristics of extreme pollution events (such as magnitude, frequency, and persistence) over Scandinavia depends largely on prevailing circulation patterns and meteorological conditions. The local meteorology can enhance or dampen the concentration of the pollutants depending on the degree of persistency; the knowledge of which would help to better constrain the chemistry transport models. Therefore, identifying the dominant weather patterns over Scandinavia especially during extreme pollution is important. However, there has not been a systematic study linking the transport events of NO<sub>2</sub> to different meteorological conditions solely from observational data over

the Scandinavian region. Therefore, the main aims of the present study are to characterize circulation regimes and meteorological conditions of extreme pollution events, and to understand to what extent they differ from climatological conditions. There are two different ways to study this co-variability solely using observational data: (1) the “top-down approach” wherein the atmospheric state is first identified and then the variability of the tracers is evaluated. This approach gives a general perspective of the distribution of tracers based on a particular weather state and (2) the “bottom-up approach” wherein the pollution episode is first identified and the weather state associated with it is studied. In this study we make use of the bottom-up approach as explained in the next section.

## 2 Data sets and methodology

The NO<sub>2</sub> tropospheric column densities from the OMI (ozone monitoring instrument) on board the EOS Aura satellite are used in this study to define and identify extreme events (Boersma et al., 2001, 2008, 2011; Bucsela et al., 2006, 2008, 2013; Lamsal et al., 2008, 2010, 2014). Eleven years (2004–2015) of daily Level 3 gridded standard product, available at 0.25 × 0.25° resolution is analysed (OMNO2d, version 3, available at: [https://disc.gsfc.nasa.gov/Aura/data-holdings/OMI/omno2d\\_v003.shtml](https://disc.gsfc.nasa.gov/Aura/data-holdings/OMI/omno2d_v003.shtml)). This particular product is used as it provides good quality OMI retrievals, already screened based on recommendations by the OMI Algorithm Team. We allowed retrievals under cloudy conditions to be analysed, not only to have robust numbers of samples but also to avoid clear-sky biases since the NO<sub>2</sub> transport is often associated with cyclonic systems that lead to increased cloudiness (Zien et al., 2014). We further tested the sensitivity of our results to using only cloud-screened retrievals, to evaluate if the selection of extreme events and associated meteorological conditions are different from those cases when retrievals under partially cloudy conditions are used.

Humidity and cloud fraction retrievals from the AIRS (atmospheric infrared sounder) instrument on board Aqua satellite are used (Chahine et al., 2006; Susskind et al., 2014; Devasthale et al., 2016). Both Aqua and Aura satellites are a part of NASA’s A-Train convoy, providing added advantage of simultaneous observations of trace gases from OMI-Aura and thermodynamical information from AIRS-Aqua. AIRS Version 6 Standard Level 3 Daily Product (AIRX3STD) for the same period (2004–2015) is used (data available at: <https://disc.gsfc.nasa.gov/ui/datasets?keywords=%22AIRS%22>).

To investigate circulation patterns, *u* and *v* wind components at 850 hPa from ECMWF’s ERA-Interim reanalysis are used (Dee et al., 2011; <http://apps.ecmwf.int/datasets/data/interim-full-daily/levtype=sfc/>).

In order to investigate co-variability of meteorological conditions and pollutants using observations, two different

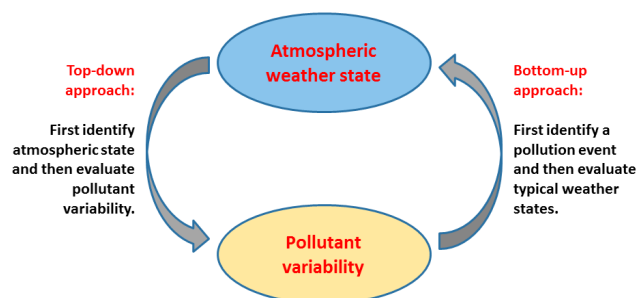


**Figure 1.** Schematic showing two different approaches to study statistical co-variability of atmospheric weather states and pollutant concentrations.

approaches can be taken (Fig. 1). In a “top-down” approach, a weather state classification can be done to identify the most prevailing weather states that occur over the study area and then the relative distribution of pollutants can be investigated under those states to rank them. This approach was adapted by Thomas and Devasthale (2014) and Devasthale and Thomas (2012). In a “bottom-up” approach on the other hand, a set of pollution events can be identified first and then the corresponding meteorological conditions can be investigated. This bottom-up approach is the focus of the present study. It should be mentioned that both of these approaches have their advantages and limitations. For example, the dominant weather pattern identified in the top-down approach may not have the largest impact on pollutant variability and the pollution events identified in the bottom-up approach may not be associated with the dominant weather pattern or may not have the largest impact on an average in the weather state they occur. Therefore, only the combination of these two approaches will provide a complete picture of the co-variability between meteorological conditions and pollutants.

In the present study, an “extreme” pollution event is defined as follows. First, the histograms of NO<sub>2</sub> tropospheric column densities using OMI data for each month are computed over the centre of the study area (55–60° N, 11–20° E). This area is chosen because it accommodates the top ten polluted and populated cities or regions in Sweden (Sjöberg et al., 2004; Klingberg et al., 2009; Bellandar et al., 2012; Gustafsson et al., 2014; Nilsson Sommar et al., 2014; Oudin et al., 2016; Taj et al., 2016). All events that surpass the 90th percentile (90 %) value are considered as extreme events. The monthly histograms of NO<sub>2</sub> over the study region are shown in Fig. 2 along with the 90th percentile thresholds for each month (vertical lines). Since NO<sub>2</sub> distributions over the study area show strong monthly variability, the monthly thresholds were chosen to define extreme events. The distributions of NO<sub>2</sub> have longer tails during the winter half-year and the tropospheric columns are also higher. Therefore, the resulting 90th percentile thresholds are also higher in winter compared to summer months. However, using thresholds based

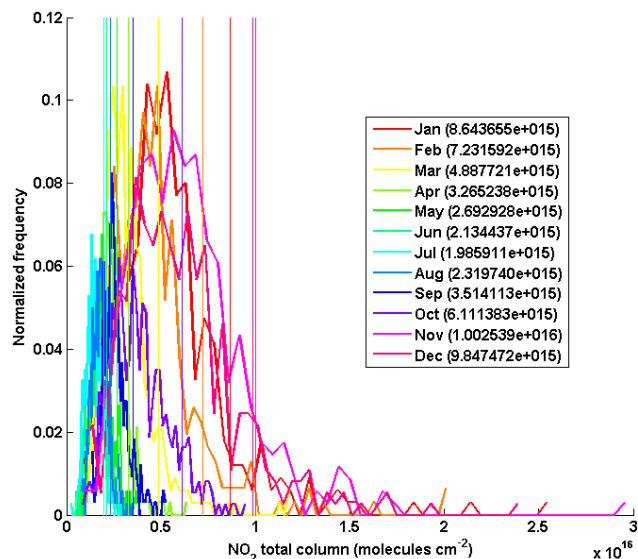


**Figure 2.** Monthly histograms of tropospheric total column NO<sub>2</sub> over the centre of the study area (55–60° N, 11–20° E) and corresponding 90th percentile thresholds (shown by vertical lines and values in brackets).

on percentiles (rather than having a fixed value throughout the season or year) makes the criteria for the selection of extreme events fair and equally applicable for each month.

### 3 Meteorological conditions observed during extreme events

The spatial distribution of tropospheric NO<sub>2</sub> column during climatological conditions, extreme events, and anomalies thereof is presented in Fig. 3. Note that although the thresholds for defining extreme events are different for each month, the results are compiled over four distinct seasons for the sake of brevity. By definition, NO<sub>2</sub> anomalies during extreme events are similar in magnitude to climatological values over Scandinavia. The spatial extent of the severity of the extreme pollutant episodes over southern Sweden is noticeable. Under climatological conditions, highest concentrations are observed over northern Germany, France, the Netherlands, and Belgium (the Benelux region). There is a good spatial coherence between NO<sub>2</sub> distributions under climatological conditions and extreme events, in the sense that the high concentrations of NO<sub>2</sub> seemed to have spread over southern Scandinavia during extreme events from the regions where climatological values are usually higher. It is to be noted that during extreme events, the pollution levels over northern European regions are also enhanced. For an event to qualify as an extreme event over southern Scandinavia, the pollutant levels in the source regions also need to be higher than usual in order to allow strong transport under favourable atmospheric circulation patterns. This provides confidence in the selec-

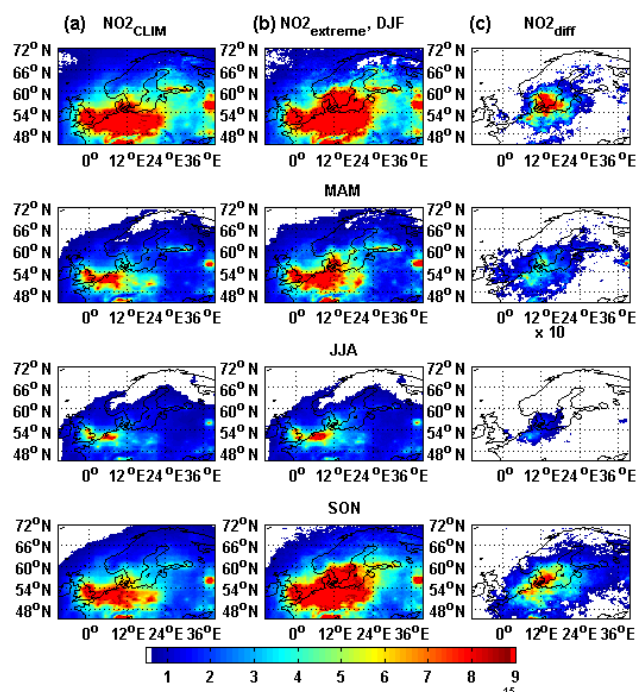


**Figure 3.** Seasonal, climatological average tropospheric NO<sub>2</sub> total column (a) based on nearly 11-year OMI data (2004–2015), NO<sub>2</sub> distribution during extreme events (b) and the difference between the two (c). The units are in molecules cm<sup>-2</sup>.

tion process of extreme events. The NO<sub>2</sub> concentrations are relatively higher in winter and autumn compared to the summer months. This is mainly because atmospheric removal by radical species and deposition are much more efficient in the summer months.

In order to characterize typical meteorological conditions that can result in such high concentrations over Scandinavia, we first investigated the dominant wind direction at 850 hPa associated with those extreme events using ERA-Interim reanalysis data. The normalized frequency of occurrence of different wind directions during the four seasons is shown in Fig. 4. It can be seen that, irrespective of the season, the south-westerly winds are dominant during extreme events accounting for 50–65 % of total events. This is consistent with the south-westerly extension of pollution plume mentioned earlier. The second largest annual occurrence is from south-easterly winds, accounting for 17 % of total events followed by an equally similar contribution from north-westerly winds. Compared to climatological conditions, south-westerly winds have 30–40 % more likelihood of being dominant during extreme events depending on the season. However, such a clear tendency compared to climatological conditions is not observed in the case of other wind directions. The spatial pattern of the 850 hPa winds based on ERA-Interim reanalysis and corresponding humidity anomalies at 850 hPa based on AIRS data during extreme events are shown in Figs. 5 and 6, respectively. A clear transport

pathway from northern continental Europe to Scandinavia is visible. The strongest winds are observed during the DJF (December, January, February) months followed by the SON months with average wind speeds reaching over 10 ms<sup>-1</sup>. The weakest winds are observed during the JJA months. The circulation pattern is characterized by the presence of low-pressure systems in the Norwegian Sea that create favourable conditions for the transport of pollutants from continental Europe into Scandinavia. The location of the centre of these cyclonic systems can slightly vary over the Norwegian Sea, affecting the direction and strength of the northward flow, as evident in Fig. 5. For example, in the DJF months, the centre is located far away in the open Norwegian Sea allowing stronger south-westerly winds over southern Scandinavia. In the JJA months, the centre of cyclonic systems is close to the western Norwegian coast. While this pattern also leads to south-westerly winds, air masses are mixed with colder and drier air from the northern Norwegian Sea.

The specific humidity anomalies show an influx of warmer and moister air masses over Scandinavia (Fig. 6), except in summer as mentioned above. The seasonality in the vertical structure of the specific humidity anomalies over Scandinavia is shown in Fig. 7c. While there are large deviations in humidity anomalies, influenced by the strength of the wind flow, they are positive regardless of the season during extreme events and peak at 2–3 km above the surface. Such an increase in the free tropospheric moisture, especially during the winter half-year in the absence of local moisture sources, can only be explained by the transport from southern latitudes. The vertical water vapour anomalies are higher in the winter half-year (DJF and SON), consistent with high NO<sub>2</sub> anomalies during those months. Figure 8 further shows cloud fraction anomalies. Average cloudiness is increased in all seasons during extreme events, in particular during the winter half-year. During this time of year, the large-scale frontal systems originating from the south-westerly regions can bring moister air masses over Scandinavia, as can be seen in the circulation patterns and humidity anomalies, creating favourable conditions for cloud formation. Therefore, these positive cloud fraction anomalies, in combination with positive humidity anomalies and circulation patterns, are indicative of the long-range transport of air masses associated with increased NO<sub>2</sub> concentrations.

For an extreme pollution event to be linked with the transport, the wind flow should be stronger allowing rapid advection and an associated circulation pattern also needs to be persistent. Figure 7a and b show the histograms of wind speed at 850 hPa over the study area during extreme events when data are partitioned by wind direction and by season, respectively. The average values of wind speeds are also shown for extreme events and climatological conditions (in brackets). Although the distributions are shifted to higher wind speeds in nearly all cases during extreme events compared to climatological conditions, the average wind speeds are not significantly different. The south-westerly winds are

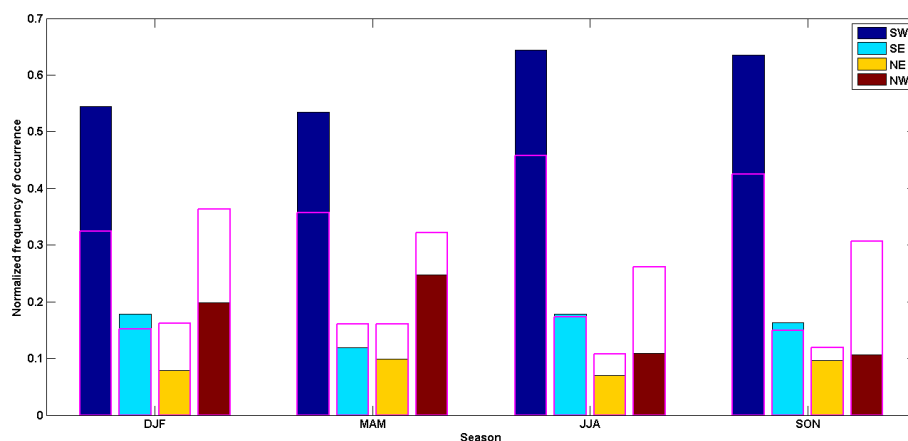


**Figure 4.** Seasonal normalized frequency of occurrence of a particular wind direction at 850 hPa when NO<sub>2</sub> extreme pollution events were observed. The hollow magenta bars show normalized frequency under climatological conditions.

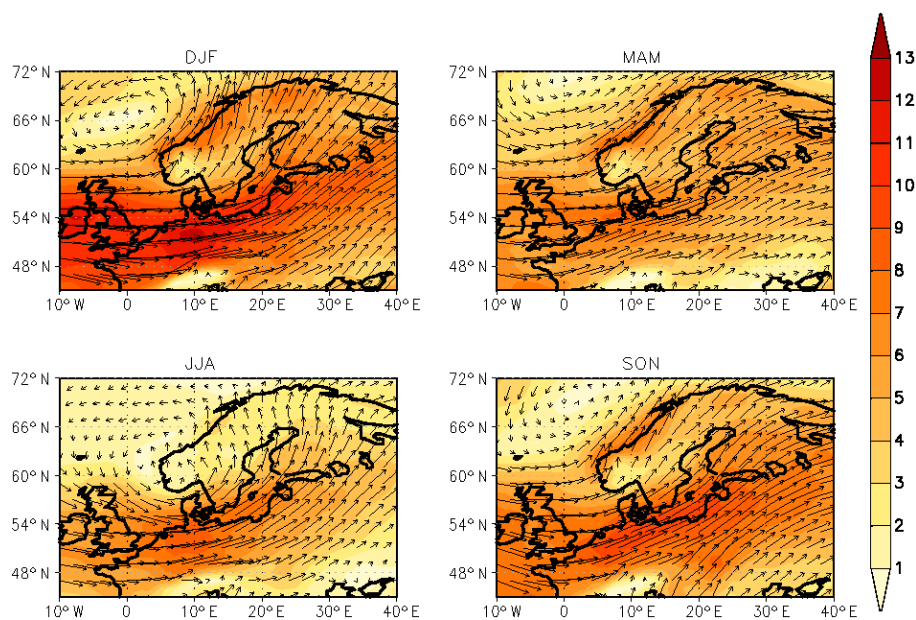


**Figure 5.** Seasonal average wind strengths and directions at 850 hPa showing the dominant circulation pattern observed when NO<sub>2</sub> extreme pollution events occur.

strongest and show the largest difference in average wind speeds, while the north-easterly winds are weakest. Average wind speeds during the winter half-year (DJF and SON) are higher than the summer half-year, consistent with observed positive anomalies of humidity and clouds.

The persistency of the different circulation patterns during these extreme events is further evaluated as shown in Fig. 7d. The persistency is defined as follows: if an extreme event is observed, the wind speed and wind direction are computed for the last 10 days. It is then checked how many days back in time that particular wind direction was *continuously* sustained and that wind direction is not changed by more than  $\pm 15^\circ$  (a third of the quadrant) during that time period. It is

to be noted that the choice of the  $\pm 15^\circ$  threshold is based on the visual inspection of about 25 test cases. It was found that if a stricter threshold is used (requiring wind direction deviations less than  $\pm 5^\circ$ ) the sampling is considerably reduced for long persistency events. On the other hand, if a more relaxed threshold is used (allowing deviations up to  $\pm 30^\circ$ ) we incorporate tail ends of the events that persisted over neighbouring areas. Two distinct modes in the persistency of circulation patterns are observed, one in which a particular wind direction persists for a day or two and a second mode in which winds persists for 3 to 5 continuous days. This is clearly different from the degree of persistency observed under climatological conditions when winds persisted in one particu-

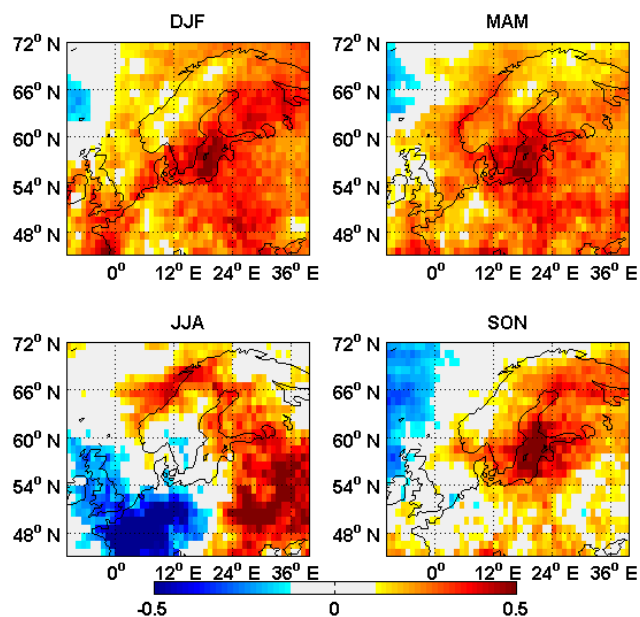


**Figure 6.** The seasonal spatial patterns of specific humidity anomalies ( $\text{g kg}^{-1}$ ) during extreme NO<sub>2</sub> pollution events.

lar direction predominantly for a few days. It was identified that during extreme events south-easterly winds dominated the first mode explaining 78 % of the total occurrence in that mode and the westerly winds dominated the second mode explaining 86 % of the total occurrence. In the latter case, when the winds persist for a few days (3–5 days), the conditions are favourable for the long-range transport from the southern latitudes since circulation patterns (Fig. 5) are associated with typical frontal systems and baroclinic disturbances that make their way over Scandinavia.

#### 4 Sensitivity of chosen events to the cloud clearing procedure

As mentioned in Sect. 2, we allowed retrievals under cloudy conditions to be analysed, not only to have a robust number of samples but also to avoid potential clear-sky biases. However, clouds can contaminate the NO<sub>2</sub> retrievals by modulating scattering in the atmosphere. Moreover, clouds are highly variable not only in space and time but also in their nature, thus making it challenging to assess their overall impact on the quality of retrievals. In the case of our study, potential cloud contamination can affect the selection of extreme events and thereby associated weather patterns that are being studied. Therefore, we carried out a sensitivity study wherein the entire analysis was repeated using only cloud-screened NO<sub>2</sub> retrievals to investigate to what extent cloud clearing would affect the chosen events and subsequent analysis. We required that the cloud fraction is less than 10 % in AIRS data and valid retrievals of OMI cloud-cleared tropospheric

column NO<sub>2</sub> are available. Figure 9 shows the histograms of NO<sub>2</sub> total columns under partially cloudy (solid lines) and cloud-screened conditions (dashed lines). The histograms are accumulated over four seasons instead of months for clarity (to avoid too many lines). The chosen 90th percentile thresholds are certainly different under partially cloudy and cloud-screened conditions, but only slightly. We also found that, depending on the month, the selected extreme events match under partially cloudy and cloud-screened conditions between 76 and 88 % of the time. Figure 10 further shows the spatial climatological distribution of NO<sub>2</sub> and its distribution during extreme events using only cloud-screened retrievals. When compared to Fig. 3, the spatial distributions look patchy as a result of selected screening but the magnitude and spatial features do not change significantly, providing confidence in our earlier analysis based on partially cloudy retrievals. Finally we evaluated if the events based on cloud-screened data impact the analysis of meteorological conditions investigated here. Figure 11 shows the vertical structure of specific humidity anomalies over the study region under partially cloudy (solid lines) and cloud-screened conditions (dashed lines). While slight differences in the vertical structure do exist, their sign and magnitudes are not large enough to change any previous arguments.

#### 5 Conclusions

The main aim of the present study was to characterize typical meteorological conditions associated with extreme NO<sub>2</sub> pollution events over Scandinavia. To that end, the study employs the bottom-up approach, in contrast to top-down approach taken by Thomas and Devasthale (2014) to study statistical co-variability of weather states and pollutant distribution. Such detailed analysis characterizing circulation patterns and meteorological conditions involving more than 300 extreme pollution events identified using satellite data has not been done before over the Scandinavian region. It is observed that the south-westerly winds dominated during extreme events accounting for 50–65 % of total events, while the second largest annual occurrence was from south-easterly winds, accounting for 17 % of total events followed by an equally similar contribution from north-westerly winds. Wind speeds are generally higher during extreme events, but only slightly, making it challenging to delineate distinct circulation regimes under these events. For the first time, we investigated the degree of persistency of wind direction during extreme events. In contrast to climatological conditions, two distinct modes of persistency were found; the first one lasting a day or so and dominated by winds from south-easterly direction and the other mode lasting 3 to 5 days dominated by the south-westerly and north-westerly winds. This information on the degree of persistency in conjunction with circulation patterns could be useful to identify extreme transport events. Further analysis of circulation patterns in combina-

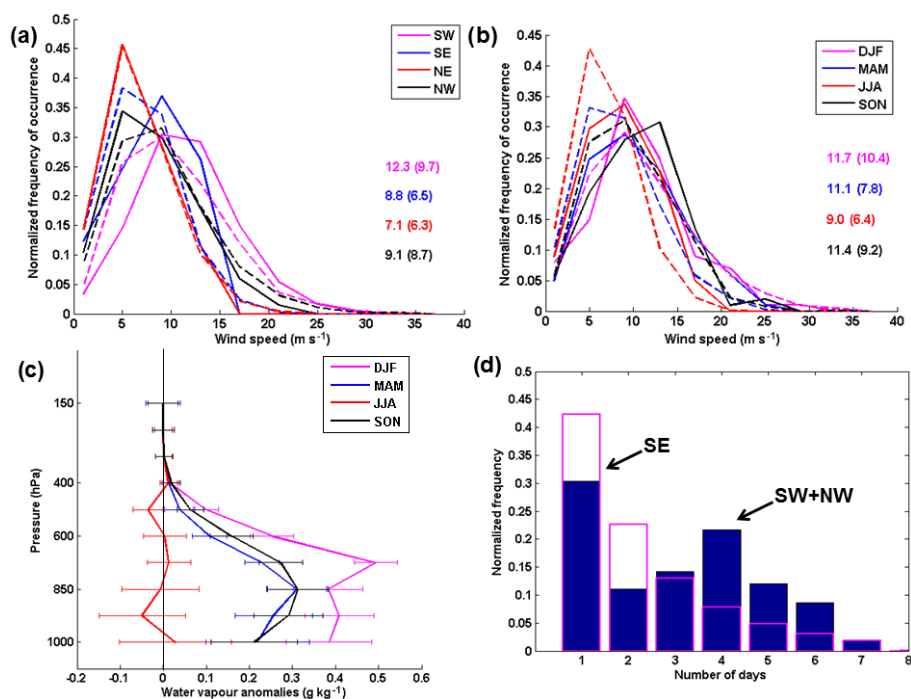


**Figure 7.** (a) Histograms of wind speeds ( $\text{m s}^{-1}$ ) at 850 hPa over the centre of the study area ( $55\text{--}60^\circ\text{N}$ ,  $11\text{--}20^\circ\text{E}$ ) during extreme events (solid lines) and climatological conditions (dashed lines, 2004–2015) when data are partitioned for different wind directions. The numbers show average wind speeds ( $\text{m s}^{-1}$ ) during extreme events and in brackets under climatological conditions. (b) Same as in (a), but when wind data are partitioned for different seasons. (c) Vertical anomalies of specific humidity ( $\text{g kg}^{-1}$ ) during extreme events with horizontal bars showing standard deviations. (d) Persistency of wind directions as a function of number of continuous days. The magenta bars show persistency under climatological conditions.

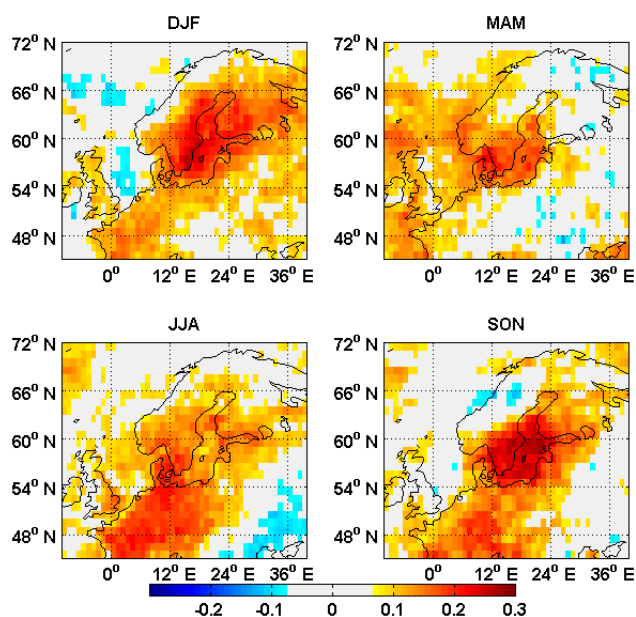


**Figure 8.** Total cloud fraction anomalies observed during extreme events based on AIRS data.

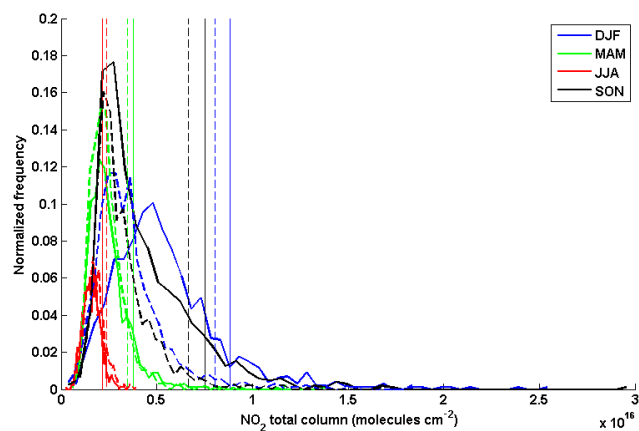


**Figure 9.** Seasonal histograms of total column tropospheric NO<sub>2</sub> over the centre of the study area ( $55\text{--}60^\circ\text{N}$ ,  $11\text{--}20^\circ\text{E}$ ) and corresponding 90th percentile thresholds (shown by vertical lines). The solid lines show histograms based on retrievals under partially cloudy conditions, while the dashed lines show histograms based only on cloud-cleared retrievals.

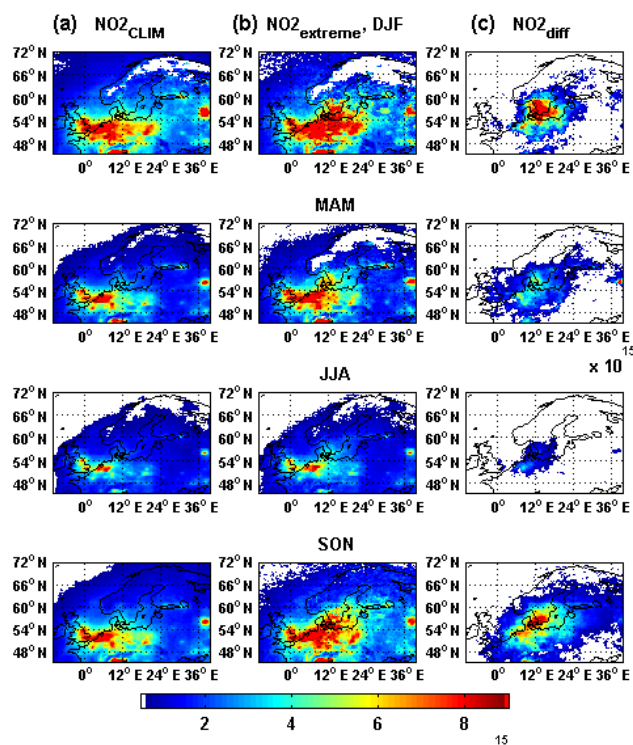


**Figure 10.** Seasonal, climatological average tropospheric NO<sub>2</sub> total column (a) based only on cloud-screened OMI data (2004–2015), NO<sub>2</sub> distribution during extreme events (b; also based on cloud-screened data) and the difference between the two (c). The units are in molecules cm<sup>-2</sup>.

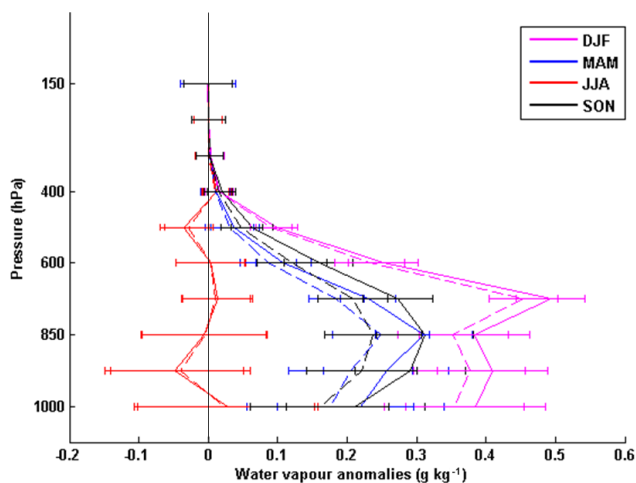


**Figure 11.** Vertical anomalies of specific humidity ( $\text{g kg}^{-1}$ ) during extreme events with horizontal bars showing standard deviations. The solid lines show anomalies under partially cloudy retrievals and dashed lines are based on cloud-screened retrievals.

tion with the spatial distribution of humidity and its vertical structure suggest that these events occur as a result of long-range transport from southern latitudes, most likely from the northern parts of Germany, France, the Netherlands, and Bel-

gium. The analysis presented here provides information that can be used in the process-oriented evaluation of chemistry transport models over Scandinavia.

**Data availability.** The datasets used in this study are publicly available at the ECMWF Data Portal (<http://apps.ecmwf.int/datasets/data/interim-full-daily/levtype=sfc/>) and NASA GES DISC ([https://disc.gsfc.nasa.gov/datasets/OMNO2d\\_V003/summary](https://disc.gsfc.nasa.gov/datasets/OMNO2d_V003/summary)).

**Competing interests.** The authors declare that they have no conflict of interest.

**Acknowledgements.** We gratefully acknowledge OMI and AIRS Science Team and NASA GES DISC for providing data. The wind data from ERA-Interim reanalysis have been obtained from the ECMWF data server. MAT acknowledges funding support from the Swedish Clean Air and climate research program of IVL (Swedish Environmental Research Institute). Both MAT and AD acknowledge the Swedish National Space Board (grants 84/11:1, 84/11:2, Dnr: 94/16).

Edited by: Thomas Wagner

Reviewed by: two anonymous referees

## References

- Beirle, S., Boersma, K. F., Platt, U., Lawrence, M. G., and Wagner, T.: Megacity Emissions and Lifetimes of Nitrogen Oxides Probed from Space, *Science*, 333, 1737–1739, <https://doi.org/10.1126/science.1207824>, 2011.
- Bellander, T., Wichmann, J., and Lind, T.: Individual Exposure to NO<sub>2</sub> in Relation to Spatial and Temporal Exposure Indices in Stockholm, Sweden: The INDEX Study, *PLoS ONE*, 7, e39536, <https://doi.org/10.1371/journal.pone.0039536>, 2012.
- Boersma, K. F., Bucsel, E. J., Brinkema, E. J., and Gleason, J. F.: NO<sub>2</sub>, available at: <http://eosps.gsfc.nasa.gov/atbd/docs/omi-trace-gas-algorithms/ATBD-OMI-04.pdf> (last access: 21 September 2001), OMI-EOS Algorithm Theoretical Basis Document: Trace Gas Algorithms: NO<sub>2</sub>, 4, 12–35, 2001.
- Boersma, K. F., Jacob, D. J., Bucsel, E. J., Perring, A. E., Dirksen, R., van der A, R. J., Yantosca, R. M., Park, R. J., Wenig, M. O., and Bertram, T. H.: Validation of OMI tropospheric NO<sub>2</sub> observations during INTEX-B and application to constrain NO<sub>x</sub> emissions over the eastern United States and Mexico, *Atmos. Environ.*, 42, 4480–4497, <https://doi.org/10.1016/j.atmosenv.2008.02.004>, 2008.
- Boersma, K. F., Eskes, H. J., Dirksen, R. J., van der A, R. J., Veefkind, J. P., Stammes, P., Huijnen, V., Kleipool, Q. L., Sneep, M., Claas, J., Leitão, J., Richter, A., Zhou, Y., and Brunner, D.: An improved tropospheric NO<sub>2</sub> column retrieval algorithm for the Ozone Monitoring Instrument, *Atmos. Meas. Tech.*, 4, 1905–1928, <https://doi.org/10.5194/amt-4-1905-2011>, 2011.
- Bucsel, E. J., Celarier, E. A., Wenig, M. O., Gleason, J. F., Veefkind, J. P., Boersma, K. F., and Brinkema, E. J.: Algo-



- rithm for NO<sub>2</sub> vertical column retrieval from the ozone monitoring instrument, *IEEE T. Geosci. Remote*, 44, 1245–1258, <https://doi.org/10.1109/TGRS.2005.863715>, 2006.
- Bucsela, E. J., Perring, A. E., Cohen, R. C., Boersma, K. F., Celarier, E. A., Gleason, J. F., Wenig, M. O., Bertram, T. H., Wooldridge, P. J., Dirksen, R., and Veefkind, J. P.: Comparison of tropospheric NO<sub>2</sub> from in situ aircraft measurements with near-real-time and standard product data from OMI, *J. Geophys. Res.*, 113, D16S31, <https://doi.org/10.1029/2007JD008838>, 2008.
- Bucsela, E. J., Krotkov, N. A., Celarier, E. A., Lamsal, L. N., Swartz, W. H., Bhartia, P. K., Boersma, K. F., Veefkind, J. P., Gleason, J. F., and Pickering, K. E.: A new stratospheric and tropospheric NO<sub>2</sub> retrieval algorithm for nadir-viewing satellite instruments: applications to OMI, *Atmos. Meas. Tech.*, 6, 2607–2626, <https://doi.org/10.5194/amt-6-2607-2013>, 2013.
- Chahine, M. T., Pagano, T. S., Aumann, H. H., Atlas, R., Barnet, C., Blaisdell, J., Chen, L., Divakarla, M., Fetzer, E. J., Goldberg, M., Gautier, C., Granger, S., Hannon, S., Irion, F. W., Kakar, R., Kalnay, E., Lambrigtsen, B. H., Lee, S.-Y., Le Marshall, J., McMillan, W. W., McMillin, L., Olsen, E. T., Revercomb, H., Rosenkranz, P., Smith, W. L., Staelin, D., Strow, L. L., Susskind, J., Tobin, D., Wolf, W., and Zhou, L.: AIRS: Improving Weather Forecasting and Providing New Data on Greenhouse Gases, *B. Am. Meteorol. Soc.*, 87, 911–926, 2006.
- Dee, D. P., Uppala, S. M., Simmons, A. J., Berrisford, P., Poli, P., Kobayashi, S., Andrae, U., Balmaseda, M. A., Balsamo, G., Bauer, P., Bechtold, P., Beljaars, A. C. M., van de Berg, L., Bidlot, J., Bormann, N., Delsol, C., Dragani, R., Fuentes, M., Geer, A. J., Haimberger, L., Healy, S. B., Hersbach, H., Hólm, E. V., Isaksen, I., Kållberg, P., Köhler, M., Matricardi, M., McNally, A. P., Monge-Sanz, B. M., Morcrette, J.-J., Park, B.-K., Peubey, C., de Rosnay, P., Tavolato, C., Thépaut, J.-N., and Vitart, F.: The ERA-Interim reanalysis: configuration and performance of the data assimilation system, *Q. J. Roy. Meteorol. Soc.*, 137, 553–597, <https://doi.org/10.1002/qj.828>, 2011.
- Devasthale, A. and Thomas, M. A.: An investigation of statistical link between inversion strength and carbon monoxide over Scandinavia in winter using AIRS data, *Atmos. Environ.*, 56, 109–114, <https://doi.org/10.1016/j.atmosenv.2012.03.042>, 2012.
- Devasthale, A., Sedlar, J., Kahn, B., Tjernström, M., Fetzer, E., Tian, B., Teixeira, J., and Pagano, T.: A decade of space borne observations of the Arctic atmosphere: novel insights from NASA's Atmospheric Infrared Sounder (AIRS) instrument, *B. Am. Meteorol. Soc.*, in press, <https://doi.org/10.1175/BAMS-D-14-00202.1>, 2016.
- Donnelly, A. A., Broderick, B. M., and Misstear, B. D.: The effect of long-range air mass transport pathways on PM<sub>10</sub> and NO<sub>2</sub> concentrations at urban and rural background sites in Ireland: Quantification using clustering techniques, *J. Environ. Sci. Health A*, 50, 7, <https://doi.org/10.1080/10934529.2015.1011955>, 2015.
- Eckhardt, S., Stohl, A., Beirle, S., Spichtinger, N., James, P., Forster, C., Junker, C., Wagner, T., Platt, U., and Jennings, S. G.: The North Atlantic Oscillation controls air pollution transport to the Arctic, *Atmos. Chem. Phys.*, 3, 1769–1778, <https://doi.org/10.5194/acp-3-1769-2003>, 2003.
- ECMWF Data Portal: ERA Interim, Daily, available at: <http://apps.ecmwf.int/datasets/data/interim-full-daily/levtype=sfc/> (last access: 12 January 2016), 2011.
- Geddes, J. A., Martin, R. V., Boys, B. L., and van Donkelaar, A.: Long-term trends worldwide in ambient NO<sub>2</sub> concentrations inferred from satellite observations, *Environ. Health Perspect.*, 124, 281–289, <https://doi.org/10.1289/ehp.1409567>, 2016.
- Gustafsson, M., Orru, H., Forsberg, B., Åström, S., Tekie, H., and Sjöberg, K.: Quantification of population exposure to NO<sub>2</sub>, PM<sub>2.5</sub> and PM<sub>10</sub> in Sweden 2010, Swedish Environmental Research Institute (IVL), IVL Report B2197, pp. 74, December 2014.
- Klingberg, J., Björkman, M. P., Karlsson, G. P., and Pleijel, H.: Observations of Ground-level Ozone and NO<sub>2</sub> in Northernmost Sweden, Including the Scandian Mountain Range, *AMBIO*, 38, 448–451, <https://doi.org/10.1579/0044-7447-38.8.448>, 2009.
- Lamarque, J.-F., Dentener, F., McConnell, J., Ro, C.-U., Shaw, M., Vet, R., Bergmann, D., Cameron-Smith, P., Dalsoren, S., Doherty, R., Faluvegi, G., Ghan, S. J., Josse, B., Lee, Y. H., MacKenzie, I. A., Plummer, D., Shindell, D. T., Skeie, R. B., Stevenson, D. S., Strode, S., Zeng, G., Curran, M., Dahl-Jensen, D., Das, S., Fritzsche, D., and Nolan, M.: Multi-model mean nitrogen and sulfur deposition from the Atmospheric Chemistry and Climate Model Intercomparison Project (ACCMIP): evaluation of historical and projected future changes, *Atmos. Chem. Phys.*, 13, 7997–8018, <https://doi.org/10.5194/acp-13-7997-2013>, 2013.
- Lamsal, L. N., Martin, R. V., van Donkelaar, A., Steinbacher, M., Celarier, E. A., Bucsela, E., Dunlea, E. J., and Pinto, J. P.: Ground-level nitrogen dioxide concentrations inferred from the satellite-borne Ozone Monitoring Instrument, *J. Geophys. Res.*, 113, D16308, <https://doi.org/10.1029/2007JD009235>, 2008.
- Lamsal, L. N., Martin, R. V., van Donkelaar, A., Celarier, E. A., Bucsela, E. J., Boersma, K. F., Dirksen, R., Luo, C., and Wang, Y.: Indirect validation of tropospheric nitrogen dioxide retrieved from the OMI satellite instrument: insight into the seasonal variation of nitrogen oxides at northern midlatitudes, *J. Geophys. Res.*, 115, D05302, <https://doi.org/10.1029/2009JD013351>, 2010.
- Lamsal, L. N., Krotkov, N. A., Celarier, E. A., Swartz, W. H., Pickering, K. E., Bucsela, E. J., Gleason, J. F., Martin, R. V., Philip, S., Irie, H., Cede, A., Herman, J., Weinheimer, A., Szykman, J. J., and Knepp, T. N.: Evaluation of OMI operational standard NO<sub>2</sub> column retrievals using in situ and surface-based NO<sub>2</sub> observations, *Atmos. Chem. Phys.*, 14, 11587–11609, <https://doi.org/10.5194/acp-14-11587-2014>, 2014.
- Miyazaki, K., Eskes, H., Sudo, K., Boersma, K. F., Bowman, K., and Kanaya, Y.: Decadal changes in global surface NO<sub>x</sub> emissions from multi-constituent satellite data assimilation, *Atmos. Chem. Phys.*, 17, 807–837, <https://doi.org/10.5194/acp-17-807-2017>, 2017.
- NASA GES DISC: OMNO2d: OMI/Aura NO<sub>2</sub> Cloud-Screened Total and Tropospheric Column L3 Global Gridded 0.25 degree × 0.25 degree V3, available at: [https://disc.gsfc.nasa.gov/datasets/OMNO2d\\_V003/summary](https://disc.gsfc.nasa.gov/datasets/OMNO2d_V003/summary), last access: 29 January 2016.
- Nilsson Sommar, J., Ek, A., Middelved, R., Bjerg, A., Dahlén, S.-E., Janson, C., and Forsberg, B.: Quality of life in relation to the traffic pollution indicators NO<sub>2</sub> and NO<sub>x</sub>: results from the Swedish GA2LEN survey, *BMJ Open Res.*, 1, e000039, <https://doi.org/10.1136/bmjresp-2014-000039>, 2014.

- Oudin, A., Bråbäck, L., Oudin Åström, D., Strömgen, M., and Forsberg, B.: Association between neighbourhood air pollution concentrations and dispensed medication for psychiatric disorders in a large longitudinal cohort of Swedish children and adolescents, *BMJ Open*, 6, e010004, <https://doi.org/10.1136/bmjopen-2015-010004>, 2016.
- Richter, A., Burrows, J. P., Nüss, H., Granier, C., and Niemeier, U.: Increase in tropospheric nitrogen dioxide over China observed from space, *Nature*, 437, 129–132, <https://doi.org/10.1038/nature04092>, 2005.
- Schaub, D., Weiss, A. K., Kaiser, J. W., Petritoli, A., Richter, A., Buchmann, B., and Burrows, J. P.: A transboundary transport episode of nitrogen dioxide as observed from GOME and its impact in the Alpine region, *Atmos. Chem. Phys.*, 5, 23–37, <https://doi.org/10.5194/acp-5-23-2005>, 2005.
- Schneider, P., Lahoz, W. A., and van der A, R.: Recent satellite-based trends of tropospheric nitrogen dioxide over large urban agglomerations worldwide, *Atmos. Chem. Phys.*, 15, 1205–1220, <https://doi.org/10.5194/acp-15-1205-2015>, 2015.
- Sjöberg, K., Haeger-Eugensson, M., Lijeberg, M., Blomgren, H., and Forsberg, B.: Quantification of population exposure to nitrogen dioxide in Sweden, Swedish Environmental Research Institute (IVL), IVL Report B1579, 31 pp., September 2004.
- Stohl, A., Huntrieser, H., Richter, A., Beirle, S., Cooper, O. R., Eckhardt, S., Forster, C., James, P., Spichtinger, N., Wenig, M., Wagner, T., Burrows, J. P., and Platt, U.: Rapid intercontinental air pollution transport associated with a meteorological bomb, *Atmos. Chem. Phys.*, 3, 969–985, <https://doi.org/10.5194/acp-3-969-2003>, 2003.
- Susskind, J., Blaisdell, J. M., and Iredell, L.: Improved methodology for surface and atmospheric soundings, error estimates and quality control procedures: the atmospheric infrared sounder science team version-6 retrieval algorithm, *J. Appl. Remote Sens.*, 8, 084994, <https://doi.org/10.1117/1.JRS.8.084994>, 2014.
- Taj, T., Stroh, E., Åström, D. O., Jakobsson, K., and Oudin, A.: Short-Term Fluctuations in Air Pollution and Asthma in Scania, Sweden. Is the Association Modified by Long-Term Concentrations?, *PLoS ONE*, 11, e0166614, <https://doi.org/10.1371/journal.pone.0166614>, 2016.
- Thomas, M. A. and Devasthale, A.: Sensitivity of free tropospheric carbon monoxide to atmospheric weather states and their persistency: an observational assessment over the Nordic countries, *Atmos. Chem. Phys.*, 14, 11545–11555, <https://doi.org/10.5194/acp-14-11545-2014>, 2014.
- van der A, R. J., Eskes, H. J., Boersma, K. F., van Noije, T. P. C., Van Roozendaal, M., De Smedt, I., Peters, D. H. M. U., and Meijer, E. W.: Trends, seasonal variability and dominant NO<sub>x</sub> source derived from a ten year record of NO<sub>2</sub> measured from space, *J. Geophys. Res.*, 113, D04302, <https://doi.org/10.1029/2007JD009021>, 2008.
- Vasilkov, A. P., Joiner, J., Oreopoulos, L., Gleason, J. F., Veeffkind, P., Bucsel, E., Celarier, E. A., Spurr, R. J. D., and Platt, S.: Impact of tropospheric nitrogen dioxide on the regional radiation budget, *Atmos. Chem. Phys.*, 9, 6389–6400, <https://doi.org/10.5194/acp-9-6389-2009>, 2009.
- Wenig, M., Spichtinger, N., Stohl, A., Held, G., Beirle, S., Wagner, T., Jähne, B., and Platt, U.: Intercontinental transport of nitrogen oxide pollution plumes, *Atmos. Chem. Phys.*, 3, 387–393, <https://doi.org/10.5194/acp-3-387-2003>, 2003.
- Zhang, Q., Streets, D. G., He, K., Wang, Y., Richter, A., Burrows, J. P., Uno, I., Jang, C. J., Chen, D., Yao, Z., and Lei, Y.: NO<sub>x</sub> emission trends for China, 1995–2004: The view from the ground and the view from space, *J. Geophys. Res.*, 112, D22306, <https://doi.org/10.1029/2007JD008684>, 2007.
- Zien, A. W., Richter, A., Hilboll, A., Blechschmidt, A.-M., and Burrows, J. P.: Systematic analysis of tropospheric NO<sub>2</sub> long-range transport events detected in GOME-2 satellite data, *Atmos. Chem. Phys.*, 14, 7367–7396, <https://doi.org/10.5194/acp-14-7367-2014>, 2014.